

# Lipid/Detergent Interaction Thermodynamics as a Function of Molecular Shape

H. Heerklotz,\* H. Binder, G. Lantzsch, and G. Klose

*Institut für Experimentelle Physik I, Universität Leipzig, Linnéstrasse 5, D-04103 Leipzig, Germany*

A. Blume

*Fachbereich Chemie, Universität Kaiserslautern, PF 3049, D-67653 Kaiserslautern, Germany*

*Received: August 2, 1996*

In dilute aqueous mixtures of the detergent  $C_{12}EO_8$  and the phospholipid POPC the phase and partition behavior as well as the transfer enthalpies of the respective molecules between the various states (monomers, bilayers, micelles) have been measured by isothermal titration calorimetry [Heerklotz et al., *J. Phys. Chem.* **1996**, *100*, 6764]. To derive more information about the molecular interpretation of the thermodynamic data, we performed additional experiments for a series of detergents,  $C_{12}EO_n$  with  $n = 3–8$  and dependent on temperature (for  $C_{12}EO_8$ ). The data can be discussed in terms of a three-stage model (bilayers, coexistence, micelles) considering nonideal mixing within the aggregates. The mixing properties are determined by packing effects controlling the hydration of the headgroups, the water exposure of the hydrocarbon core, and the order of the hydrocarbon chains. Additionally, two types of systematic deviations from the simple three-stage behavior are found for low  $n$  and low detergent contents in the bilayer. These effects could be related to special properties of detergents surrounded by lipids only and to solubilization intermediates occurring close to the lytic detergent content.

## 1. Introduction

Recently, we presented a number of experimental protocols to investigate dilute aqueous lipid–detergent mixtures by means of isothermal titration calorimetry.<sup>1,2</sup> The transfer of detergent between water, micelles, and lipid bilayers could be specified in terms of the corresponding changes in molar enthalpy and, using suitable models, standard chemical potential.

In the frame of the three-stage model according to Lichtenberg,<sup>3,4</sup> the phase state of a dilute aqueous lipid–detergent mixture depends only on the effective detergent mole fraction in aggregates (bilayers and/or micelles),  $X_e$ . For a given total detergent mole fraction in the sample,  $X$ , the effective content  $X_e$  is a function of the partition coefficient and of the absolute lipid concentration, because the detergent monomers in the water do not contribute to  $X_e$ . The sample contains mixed bilayers up to a saturating fraction  $X_e = X_{sat}$ , and then reaches a range of coexistence of detergent-saturated bilayers ( $X_{sat}$ ) and lipid-saturated micelles (detergent content  $X_{sol}$ ) up to  $X_e = X_{sol}$ , whereas beyond  $X_{sol}$  only mixed micelles occur.

For the solubilization experiment, the cell is filled with lipid vesicles and micellar detergent solutions are injected. A sufficiently high lipid concentration is chosen to ensure that the concentration of detergent monomers can be neglected, so that the current total sample composition during the titration,  $X$ , is just equal to the effective fraction  $X_e$ . Then, special breakpoints of the titration heat can be directly related to the crossing of the phase boundaries  $X_{sat}$  and  $X_{sol}$ . Furthermore, the heat of transfer for the detergent from micelles to bilayers is obtained as a function of bilayer composition.

In our recent publication,<sup>2</sup> we suggested that the heats of transfer determined for  $C_{12}EO_8$  are correlated to changes in headgroup hydration. The main aim of this work is to derive more information about the interpretation of the thermodynamic transfer data by investigating a homologous series of detergents

$C_{12}EO_n$  ( $n = 3–8$ ) and the temperature dependence of the heats of transfer in the system  $C_{12}EO_8$ /POPC. Both parameters, the number of ethylene oxide units per detergent ( $n$ ) and the temperature ( $T$ ), cause a systematic change of the molecular shape of the detergents. Thus, whereas, e.g.,  $C_{12}EO_3$  is of approximately cylindrical shape at room temperature, the molecular asymmetry (spontaneous curvature) increases with  $n$  and decreases with  $T$ .<sup>5–7</sup>

Most of the data observed are consistent with the simple three stage model of solubilization (bilayers, coexistence, micelles)<sup>2,3</sup> considering nonideal lipid–detergent interactions within the mixed bilayers.<sup>2,8</sup> Accordingly, the variations of the phase boundaries  $X_{sat}$  and  $X_{sol}$  as well as of the nonideality parameters can be interpreted fairly well in terms of the molecular packing concept.<sup>5,9</sup>

Two types of systematic deviations of the data from the model predictions are discussed to be related to specific interactions and to effects occurring when the system approaches the lytic detergent content  $X_{sat}$ . Epand and Epand<sup>10</sup> reported that the enthalpy of incorporation of low amounts of lyso-PC into lipid bilayers depends on the curvature strain of the lipid vesicles. The exothermic contribution to the transfer heats found upon incorporation of low contents of  $C_{12}EO_n$  with  $n = 3–6$  into POPC bilayers is qualitatively and quantitatively similar to the effects occurring with Lyso-PC and MeDOPE.<sup>10</sup>

## 2. Experimental Section

1-Palmitoyl-2-oleoylphosphatidylcholine (POPC) was purchased from Avanti Polar Lipids Inc., USA. The detergents  $C_{12}EO_n$  with  $n = 3–8$  were from Nikko Chem. Ltd., Japan. The substances were used without further purification. Aqueous dispersions of the phospholipid were prepared by mixing the appropriate amounts of the lipid with purified water and subsequent vortexing. Because the lipid as well as the detergent are nonionics, no buffer was used.

\* Corresponding author. E-mail: HEERKLOT@RZ.UNI-LEIPZIG.DE.  
Fax +49-341-97 32474.

† Abstract published in *Advance ACS Abstracts*, December 15, 1996.

Large unilamellar lipid vesicles of 100 nm diameter were obtained by the extrusion method using the device from Lipex Biomembranes Inc., Canada, with Nuclepore Inc. polycarbonate membranes (10 times each sample).

The isothermal titration calorimetry experiments were carried out with an MCS ITC, MicroCal, USA,<sup>11</sup> and evaluated using the MicroCal Origin software. The sample cell has a volume of 1.34 mL.

Special stirring syringes with 60, 130, and 300  $\mu\text{L}$  volume are used for the injections. Prior to the experiment, the titrant as well as the cell content were degassed at 3 kPa for 10 min to prevent air bubbles. A preliminary injection of 1  $\mu\text{L}$  is used to cover the enhanced error of the first injection, which is due to a possible slight loss of titrant upon mounting the syringe. The material preliminarily injected is considered in the concentration scale, but not for the measured reaction heat. All data are automatically corrected for sample replacement by the injected titrant volume.

The ITC solubilization experiment with detergent titration<sup>2</sup> was done for each of the detergents investigated. 100 mM micellar detergent solutions were titrated to 5 mM POPC LUV suspensions. Only the experiments for  $\text{C}_{12}\text{EO}_3$  and  $\text{C}_{12}\text{EO}_4$  (cf. Figure 5) were done with 2.5 mM POPC and 40 mM detergent which is sufficient because of the higher partition coefficients of these detergents. The data were obtained by a combination of experiments using the various injection syringes of different total volume to enhance the resolution in the low titrant concentration range. On the basis of the literature<sup>12,13</sup> and our own observations,<sup>2,8</sup> we may assume that there is a fast complete equilibration of the system after injection of  $\text{C}_{12}\text{EO}_n$  detergents. Consequently, locally higher detergent concentrations which might occur during the injection are balanced quickly and do not influence the state of the system reached in the time scale of the measurement (e.g. 10 min).

### 3. Results

**3.1. Solubilization Experiment.** The solubilization experiment with detergent titration to lipid vesicles<sup>1</sup> was explained in detail before.<sup>2</sup> Figure 1 illustrates the experimental raw data (titration heat power vs time) for the example of the  $\text{C}_{12}\text{EO}_8$  solubilization experiment at 10  $^\circ\text{C}$  using the 60  $\mu\text{L}$  syringe (Figure 1A) and the 300  $\mu\text{L}$  syringe (Figure 1B), respectively. The corresponding molar titration heat data ( $q_{\text{obs}}$ ) are plotted vs the total mole fraction of detergent in the sample cell ( $X$ ), which is reached during the respective injections (Figure 1C). The lipid concentration in the cell was chosen 2 orders of magnitude higher than the cmc of the detergent to ensure that aqueous detergent monomers are negligible and the effective detergent content in the membrane and/or micelles ( $X_e$ )<sup>3,4</sup> can be approximated by the total  $X$ .

The phase boundaries between the lamellar, the lamellar + micellar coexistence, and the micellar range, corresponding to the values  $X_{\text{sat}}$  and  $X_{\text{sol}}$ , are clearly indicated by breakpoints of the  $q_{\text{obs}}(X)$  plot (cf. arrows in Figure 1C).<sup>1,2</sup>

The  $q_{\text{obs}}(X)$  measured within the lamellar range ( $X < X_{\text{sat}}$ ) is just the molar transfer heat  $q_{\text{D}}^{\text{b/m}}$  of the detergent from the micelles injected to mixed bilayers of composition  $X$ .<sup>2</sup> The decrease of  $q_{\text{D}}^{\text{b/m}}$  vs  $X$  is due to nonideal mixing of detergent and lipid in the lamellae and can be modeled fairly well analogously to the regular solution model (cf. solid line in Figure 1C):

$$q_{\text{D}}^{\text{b/m}}(X) = \rho^0(1 - X_e)^2 + q_{\text{D}}^{\text{b/m}}(X_e \rightarrow 1) \quad (1)$$

where  $\rho^0$  denotes the nonideality parameter and  $q_{\text{D}}^{\text{b/m}}(1)$  the

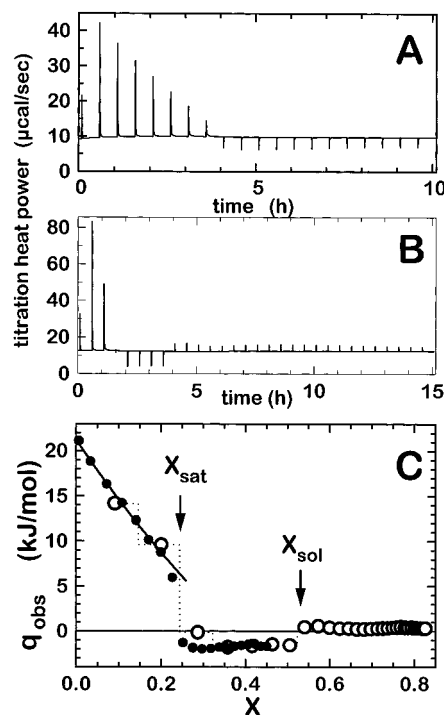


**Figure 1.** Raw data of the ITC solubilization experiment titrating a 100 mM micellar dispersion of  $\text{C}_{12}\text{EO}_8$  to a 5 mM POPC LUV suspension at 10  $^\circ\text{C}$  using 3  $\mu\text{L}$  injections out of the 60  $\mu\text{L}$  syringe (A) and 10  $\mu\text{L}$  injections out of the 300  $\mu\text{L}$  syringe (B). The detergent concentrations reached finally are 4 mM (A) and 18.7 mM (B). Injections were done every 30 min. (C) Normalized titration heat data  $q_{\text{obs}}$  corresponding to (A) (●) and (B) (○) vs the detergent mole fraction  $X$  in the sample. The line corresponds to eq 1 with  $\rho^0 = 35.3$  kJ/mol and  $q_{\text{D}}^{\text{b/m}}(1) = -13.9$  kJ/mol.

transition heat of detergent from micelles to hypothetical pure detergent bilayers.

In the frame of this model, heats of transfer to or from the water are neglected. We calculated the contribution to the observed heat which is caused by a release of detergent molecules injected as micelles to the water considering the partition coefficient and the demicellization heat for  $\text{C}_{12}\text{EO}_8/\text{POPC}$  at 25  $^\circ\text{C}$ .<sup>2</sup> In this case, this demicellization effect yields heats less than  $-1$  kJ/mol (exothermic). For temperatures above 25  $^\circ\text{C}$  and for lower  $n$  the partition coefficients are higher and the demicellization heats are lower, both causing this demicellization heat contribution to be lower. Only for the  $\text{C}_{12}\text{EO}_n$  data measured at temperatures below 25  $^\circ\text{C}$  should this error source become more pronounced which could at least partially explain the exothermic deviation of the 10  $^\circ\text{C}$  data in Figure 3 from the linear behavior.

**3.2. Temperature Dependence.** The ITC solubilization experiment was performed by titrating  $\text{C}_{12}\text{EO}_8$  micelles to POPC vesicles at various temperatures (cf. Figure 2, for example). Generally, the lytic detergent fraction  $X_{\text{sat}}$  increases from 0.25 at 10  $^\circ\text{C}$  up to 0.68 at 75  $^\circ\text{C}$ . Analogously, the limiting detergent content within mixed micelles,  $X_{\text{sol}}$ , increases with temperature.

The nonideality parameter ( $\rho^0$ ) decreases from +10 kJ/mol at 10  $^\circ\text{C}$  to zero at about 50  $^\circ\text{C}$ . Beyond 50  $^\circ\text{C}$ , the data exhibit systematic differences from the model given by eq 1, especially at low  $X$ . Figure 3 shows the heats of transfer for the detergent from micelles to pure lipid bilayers  $q_{\text{D}}^{\text{b/m}}(X \rightarrow 0)$  and to detergent-saturated bilayers  $q_{\text{D}}^{\text{b/m}}(X \rightarrow X_{\text{sat}})$  vs temperature  $T$ , which are given as the limiting values of the titration heats for  $X \rightarrow 0$  and for  $X \rightarrow X_{\text{sat}}$  (cf., e.g., Figure 2). At least within the temperature range 20–50  $^\circ\text{C}$ , both values depend linearly on temperature.

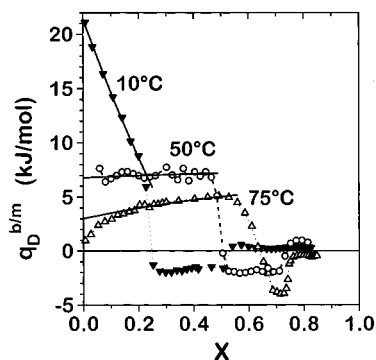


**Figure 2.** Results of the ITC solubilization experiment (cf. Figure 1) with  $C_{12}EO_8$  titrated to POPC LUV as a function of temperature: at 10 °C ( $\blacktriangledown$ ), 50 °C ( $\circ$ ) and 75 °C ( $\triangle$ ). The solid model lines correspond to eq 1.

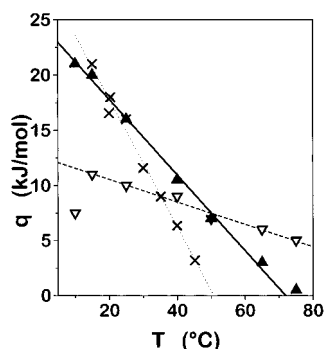


**Figure 3.** Heats of transfer of  $C_{12}EO_8$  from micelles to pure POPC bilayers ( $X \rightarrow 0$ ,  $\blacktriangle$ ) and to detergent-saturated bilayers ( $X \rightarrow X_{\text{sat}}$ ,  $\nabla$ ) and the heats of micelle formation ( $\times$ ). The data were derived from the ITC demicellization experiment (not shown in detail) and the solubilization experiment, respectively, for example cf. Figure 2. The parameters of the linear regressions are given in the text. Note that the experimental error is higher for data measured below 25 °C (cf. section 3.1).

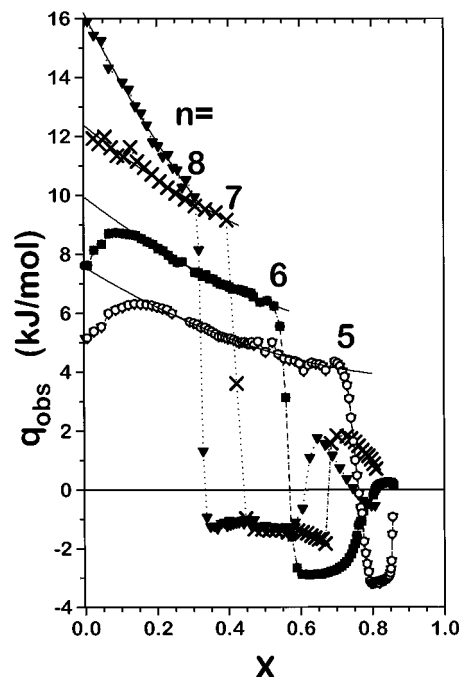
The difference of the molar heat capacity of the detergent between the bilayer and the micellar state ( $\Delta C_p^{b/m}$ ) is the derivative of the heat of transfer with respect to temperature,  $\Delta q_D^{b/m}/\Delta T$ , i.e., the slope of the plots in Figure 3. Linear regression yields  $\Delta C_p^{b/m}(X \rightarrow 0) = -0.32 \pm 0.02$  kJ/(mol K) and  $\Delta C_p^{b/m}(X \rightarrow X_{\text{sat}}) = -0.11 \pm 0.01$  kJ/(mol K) for the linear range between 20 and 65 °C.

The heats of micelle formation of  $C_{12}EO_8$ , which are derived from the ITC demicellization experiment (cf. ref 2 for  $C_{12}EO_8$  at 25 °C) are shown for comparison (crosses in Figure 3). Note that the micelle formation heats just differ in sign from the demicellization heats measured. The corresponding heat capacity change is  $\Delta C_p^{m/w} = -0.6$  kJ/(mol K).

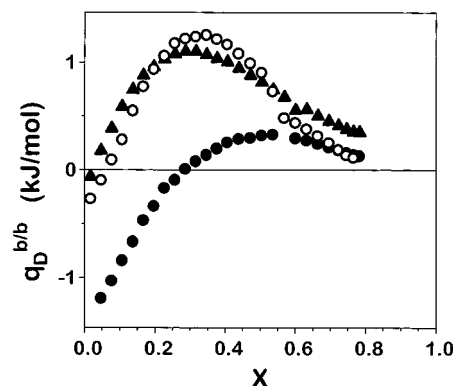
**3.3. Variation of the Number of EO Groups per Detergent.** The detergents  $C_{12}EO_n$  with  $n = 5-8$  form micelles in dilute aqueous solutions at 25 °C<sup>14,15</sup> the cmc changing from about 70  $\mu\text{M}$  for  $C_{12}EO_5$  to 90  $\mu\text{M}$  for  $C_{12}EO_8$ .<sup>2,8</sup>

Figure 4 shows the results of solubilization experiments based on the titration of a 100 mM micellar detergent solution to 5 mM LUV of POPC for  $C_{12}EO_n$  with  $n = 5-8$  at 25 °C. Generally, the decrease of the number of EO units per detergent ( $n$ ) leads to an increase in the limiting detergent mole fractions  $X_{\text{sat}}$  and  $X_{\text{sol}}$  and to decreasing nonideality parameters. For  $n \leq 6$ , systematic exothermic deviations from the model behavior according to eq 1 occur at low  $X$ .

For the detergents  $C_{12}EO_n$  with  $n = 3, 4$ , this type of experiment yields results (cf. Figure 5) that are qualitatively different from the behavior observed for the others with  $n = 5-8$  (cf. Figure 4). This is due to the fact that  $C_{12}EO_3$  and



**Figure 4.** Results of the ITC solubilization experiments titrating 100 mM micellar solutions of detergents  $C_{12}EO_n$  ( $n$  values indicated in the plot) to 5 mM POPC LUV at 25 °C. The final detergent concentration is about 27 mM. The solid lines illustrate the behavior according to eq 1. For interpretation cf. section 3.1.



**Figure 5.** Titration heats for the titration of lamellar detergent suspensions to 2.5 mM POPC lamellae (vesicles) vs detergent mole fraction  $X$  with  $C_{12}EO_3$  at 25 °C ( $\bullet$ ) and at 11 °C ( $\circ$ ) and for  $C_{12}EO_4$  at 25 °C ( $\blacktriangle$ ). The final detergent concentration reached after the titration is about 8 mM.

$C_{12}EO_4$  form lamellae in aqueous solution at room temperature.<sup>14</sup> Consequently, upon detergent titration the system transforms rather gradually from lipid controlled to the detergent-controlled lamellae, and no transition to the micellar phase accompanied by breakpoints of the titration heat occurs. Furthermore, the heats measured for the detergent transfer from detergent bilayers to mixed bilayers,  $q_D^{b/b}(X)$ , are much lower than the respective data for the micellar detergents,  $q_D^{b/m}(X)$ .

## 4. Discussion

**4.1. Molecular Packing.** The detergents  $C_{12}EO_n$  with  $n = 5-8$  are characterized by the shape of a truncated cone,<sup>6</sup> because the lateral area occupied by the hydrated headgroup (e.g., 55  $\text{\AA}^2$  for  $C_{12}EO_5$ ) is larger than the optimum interfacial area per hydrocarbon chain (about 27  $\text{\AA}^2$  in liquid crystalline phase).<sup>9</sup> This lateral mismatch can be treated in terms of the molecular shape concept developed by Israelachvili<sup>9</sup> or by means of a

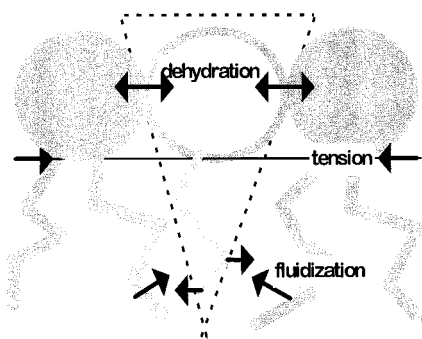


**Figure 6.** Schematic illustration of the packing mismatch of a truncated cone-shaped detergent incorporated into a lipid lamella (cf. ref 6). The consequences are a lateral headgroup compression by dehydration as well as a fluidity driven lateral area expansion per hydrocarbon chain.

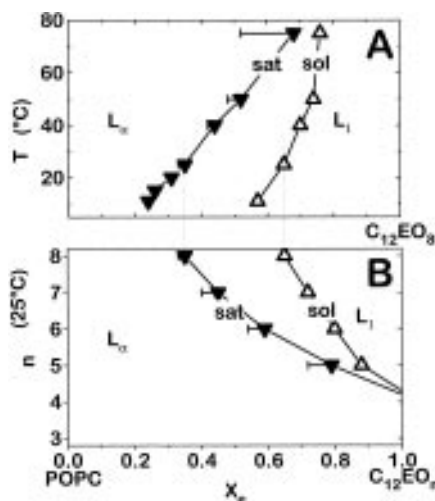


**Figure 7.** (A) Dependence of the phase boundaries  $X_{\text{sat}}$  and  $X_{\text{sol}}$  of dilute aqueous POPC/ $\text{C}_{12}\text{EO}_8$  mixtures on temperature. (B) Dependence of the  $X_{\text{sat}}$  and  $X_{\text{sol}}$  values on EO number  $n$  (cf.  $\text{C}_{12}\text{EO}_n$ ) at 25 °C. The abscissa  $X_e$  gives the mole fraction of the respective detergent within the lipid/detergent mixed aggregates. The lamellar phase is denoted  $L_\alpha$ , the micellar one  $L_1$ , between the sat and sol boundaries there is a lamellar/micellar coexistence. A micellar second-order transition<sup>2,15,17,18</sup> is not included in the plot. Error bars indicate the width of the sat boundary (cf. section 4.4).

positive spontaneous membrane curvature in the frame of the membrane elasticity model.<sup>16</sup>

Figure 6 illustrates the packing effects induced by the incorporation of a cone-shaped detergent into a lipid bilayer. In order to fit the lamellar packing, the molecular asymmetry of the detergent must be compensated by lateral headgroup compression (dehydration) and lateral hydrocarbon chain expansion (fluidization). The curvature strain within the membrane should become less pronounced (i) with increasing temperature due to headgroup dehydration and chain fluidization;<sup>6,7</sup> (ii) with a reduction of the number of ethylene oxide units per detergent headgroup, and (iii) with decreasing detergent content  $X_e$  in the membranes, because the detergent asymmetry can be compensated to some extent by neighboring lipid molecules (cf. Figure 6).<sup>6,7</sup>

These packing constraints can at least qualitatively explain the fact that the phase boundaries ( $X_{\text{sat}}$  and  $X_{\text{sol}}$ , cf. Figure 7) as well as the mixing nonideality (parameter  $\rho^0$ , compare Figures 2 and 4 and consider Figure 5) are affected very similarly by increasing temperature and by decreasing EO number,  $n$ . Our results shown in Figure 7B are in accord with the general behavior found by Partearroyo et al.<sup>19</sup> for a homologous series of Triton detergents in mixtures with EYPC. They report that

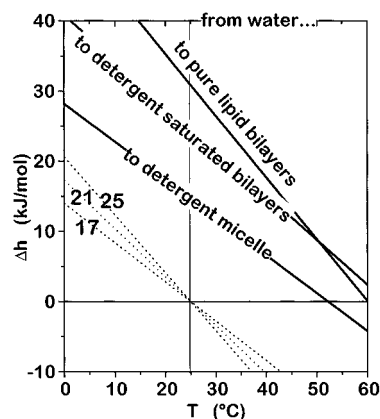


**Figure 8.** Transfer heats for the detergent from water to the aggregates specified in the plot (solid lines) vs temperature calculated using the data of Figure 3. For comparison, the enthalpies of transfer of hydrocarbon chains (dashed) with 17, 21, and 25 hydrogen atoms (cf. numbers in the plot) from water to a hydrocarbon phase are simulated.<sup>21</sup>

the lytic detergent content  $X_{\text{sat}}$  decreases continuously with increasing number of EO units per detergent, tending to about  $X_{\text{sat}} \approx 0.3$  for the most asymmetric ones. The only exception, the detergent X-305 with 30 EO groups, should be explainable by the fact that not all of these many EO groups contribute to the effective molecular asymmetry between hydrophobic core and lipid headgroup region as illustrated in Figure 6.

Vollmer and Strey<sup>20</sup> determined the transfer enthalpies of the temperature driven lamellar to microemulsion transitions ( $L_1 \rightarrow L_\alpha \rightarrow L_2$ ) for the  $\text{C}_{12}\text{EO}_5$ /octane/water system. They report values of up to  $+1 k_B T$  per surfactant (about  $+2.6 \text{ kJ/mol}$ ) for the  $L_1 \rightarrow L_\alpha$  as well as for the  $L_\alpha \rightarrow L_2$  transition, which are comparable to the heats measured here for the isothermal transfer of  $\text{C}_{12}\text{EO}_5$  from micelles to lamellae of about  $+5 \text{ kJ/mol}$ . They calculated that both the phase boundaries as well as the transfer heats are determined by the bending free energy merely, whereas all other contributions are negligible. This is quite equivalent to our packing considerations.

**4.2. Molecular Origin of the Transfer Heats.** The heat effects accompanying the hydrophobic effect, i.e., the solution of hydrocarbons in water, have been studied in detail by Gill and Wadsö.<sup>21</sup> They found that the transfer enthalpies of hydrocarbons to the water ( $\Delta h_{\text{HC}}^{\text{w/hc}}$ ) increase linearly with the temperature ( $T$ ) according to the general relation

$$\Delta h_{\text{HC}}^{\text{w/hc}} = \Delta C_p^{\text{w/hc}} (T - T^*) \quad (2)$$

The slope, i.e., the respective molar heat capacity change  $\Delta C_p^{\text{w/hc}}$ , was observed to be proportional to the number of hydrogen atoms ( $n_H$ ) which become exposed to the water by the transfer:

$$\Delta C_p^{\text{w/hc}} = n_H \times 33 \text{ J/(mol K)} \quad (3)$$

The characteristic temperature  $T^*$  corresponding to  $\Delta h_{\text{HC}}^{\text{w/hc}} = 0$ , i.e., a vanishing heat effect upon transfer of the hydrocarbon into water, was found in a relative narrow temperature range of 22–25 °C for all the hydrocarbons investigated. The temperature dependence of the transfer enthalpy from water to hydrocarbon,  $h_{\text{HC}}^{\text{hc/w}}$ , according to eq 2 (sign changes with transfer direction), is illustrated in Figure 8 for  $n_H = 17, 21$ , and 25 (dotted lines).

Also for the SDS micelle formation a linear dependence  $\Delta h(T)$  obeying  $T^* \approx 25 \text{ °C}$  was measured.<sup>22</sup> This behavior was completely interpreted in terms of the hydrophobic effect accompanying the transfer of a  $\text{C}_8\text{H}_{17}$  chain from water to the

hydrophobic core of the micelle by means of eqs 2 and 3. Consequently, it was concluded that about four methylene groups per SDS molecule remain exposed to the water also within a micelle.

We calculated the heats regarding to the transfer of  $C_{12}EO_n$  from water to bilayers according to the general rule that the thermodynamic potential differences between the b, m, and w states vanish for closed loops (e.g., Born–Haber cycles), e.g.

$$q^{b/w} = h^b - h^w = q^{b/m} + q^{m/w} \quad (4)$$

basing on the data given in Figure 3. The results are presented as solid lines in Figure 8.

The considerable upward shifts of  $T^*$  from the values observed for pure hydrocarbons to 50 °C for micelles and beyond 60 °C for detergent-saturated and pure lipid bilayers, respectively, indicate that not only the hydrocarbon chains but also the EO headgroups contribute to the transfer enthalpies.<sup>23</sup>

The slopes of the solid lines in Figure 8 correspond to a number of hydrogen atoms of  $n_H \approx 16$  (for micelles),  $n_H \approx 19$  (detergent-saturated bilayers), and  $n_H \approx 27$  (pure lipid bilayers) according to eq 3. The first and second values are equivalent to 4.5 and 3 aliphatic methylene groups per detergent being exposed to water, respectively. These values are reasonable in comparison with the respective data obtained for other detergents ( $\sim 3$ – $4$ )<sup>22</sup> and taking into account the fact that bilayers exhibit a lower relative hydrocarbon–water interface than micelles. Consequently, the contributions of the EO headgroups to the transfer heats for micelles and for detergent-saturated bilayers are almost independent of temperature and amount to about 15 and 25 kJ/mol, respectively. This result can be explained by the fact that both types of aggregates have a degree of freedom (shape and size of the micelles and composition of the detergent-saturated bilayers) to balance possible temperature-dependent curvature strains, minimizing changes of the headgroup hydration (cf. Figure 7).

The number of hydrogen atoms of the detergent affected by the hydrophobic effect in pure lipid bilayers,  $n_H = 27$ , calculated formally from eq 3 is rather unlikely even if one takes into account that an additional screening of methylene groups of the lipid from water induced by detergent incorporation could contribute to  $n_H$  in addition to the  $n_H \leq 25$  of the detergent. Hence, part of the negative slope of the transfer heat vs temperature could not be explained by the hydrophobic effect, but should be a consequence of a decrease of the headgroup effects with increasing temperature. Such a tendency would be in accord with the expectation that the curvature strain induced by the detergent cannot be balanced within a lipid lamella but causes a gradual dehydration of the detergent headgroup.

Summarizing, we emphasize that the transfer heats measured at 25 °C contain nearly no contributions from the hydrocarbon chain but reflect headgroup effects, which can be interpreted in terms of a gradual dehydration of the headgroups by the packing pressure acting on them.

**4.3. Thermodynamic Potentials as a Function of  $n$ .** A complete thermodynamic characterization of the system has to include enthalpic as well as entropic effects, because both contribute to the chemical potential differences. The enthalpy changes are heat effects measured directly, while the standard chemical potential differences  $\Delta\mu^\circ$  of the detergent between various phases can be deduced from the equilibrium state observed for the system (e.g., partition coefficients, cmc).

Figure 9 shows the standard chemical potential changes  $\Delta\mu^\circ$ , the enthalpy changes (transfer heats  $q$ ), and entropy changes (given as  $-T\Delta s$ ) for transfer of detergent monomers to micelles

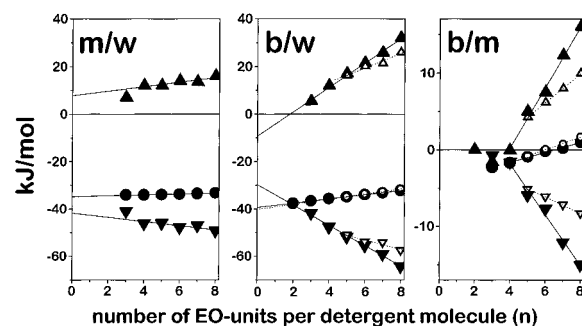


**Figure 9.** Changes of the enthalpy ( $\blacktriangle$ ,  $\triangle$ ), the entropy (given as  $-T\Delta s$ ,  $\nabla$ ,  $\triangledown$ ) and the standard chemical potential ( $\bullet$ ,  $\circ$ ) upon detergent transfer of monomers to micelles (m/w) and to bilayers (b/w) and from micelles to bilayers (b/m). In the parts labeled b/w and b/m, solid symbols denote limiting values for pure lipid bilayers and open symbols refer to detergent-saturated bilayers ( $X_{\text{sat}}$ ). The regression parameters for the experimental data are given in Table 1. The enthalpy data are based on the ITC solubilization experiment ( $q_D^{b/m}$ ) and demicellization experiment ( $-q_D^{m/w}$ , see ref 2 for  $C_{12}EO_8$ ; others not shown in detail). The standard chemical potential data are deduced from the cmc ( $\Delta\mu_D^{m/w} = -RT \ln(W/\text{cmc})$ ) (cf. ref 8 and references therein) and the partition coefficients ( $\Delta\mu_D^{b/w} = -RT \ln P$ ).<sup>8</sup> These data enable one to deduce also  $\Delta\mu_D^{b/m}$  and  $q_D^{b/w}$  analogously to eq 4. For  $C_{12}EO_8$  these values were measured independently to prove this procedure.<sup>2</sup> Finally, the entropy data were determined using  $-T\Delta s = \Delta\mu^\circ - \Delta h$ .

**TABLE 1: Linear Regression Parameters for the Experimental Data of Transfer Heats ( $q$ ) and Standard Chemical Potential Differences ( $\Delta\mu^\circ$ ) Shown in Figure 9<sup>a</sup>**

| row |  | slope<br>(kJ/(mol $n$ )) | intercept<br>(kJ/mol) | linear<br>range $n$ |
|-----|--|--------------------------|-----------------------|---------------------|
| 1   | $q_D^{b/m}(X \rightarrow 0)$           | $4.0 \pm 0.2$            | $-16 \pm 1$           | 4–8                 |
| 2   | $q_D^{b/m}(X_{\text{sat}})$            | $1.9 \pm 0.03$           | $-5.2 \pm 0.2$        | 5–8                 |
| 3   | $q_D^{m/w}$                            | $1.0 \pm 0.3$            | $8 \pm 2$             | 4–8                 |
| 4   | $\Delta\mu_D^{b/w}(X \rightarrow 0)^8$ | $0.9 \pm 0.1$            | $-39.4 \pm 0.1$       | 2–8                 |
| 5   | $\Delta\mu_D^{b/w}(X_{\text{sat}})^8$  | $1.1 \pm 0.1$            | $-40.3 \pm 0.2$       | 5–8                 |
| 6   | $\Delta\mu_D^{m/w}$                    | $0.2 \pm 0.03$           | $-34.8 \pm 0.2$       | 3–8                 |

<sup>a</sup> Rows 1 and 2 refer to the transfer heats of the detergent from micelles (for  $n = 3, 4$ : bilayers) to pure lipid membranes and to detergent-saturated membranes, respectively. Row 3 describes the heats of micelle formation. Rows 4 and 5 give the standard chemical potential differences upon detergent transfer from water to membranes basing on partitioning experiments and row 6 the respective data for micelle formation derived from the cmc.

(micelle formation, Figure 9, m/w) and to bilayers (partitioning, Figure 9, b/w) as well as for the detergent transfer from micelles (for  $n = 3, 4$ : from pure detergent bilayers) to mixed bilayers (Figure 9, b/m), as a function of the number of EO units per detergent ( $n$ ). Because the bilayer data depend also on the composition, the limiting values were given for detergent saturated ( $X \rightarrow X_{\text{sat}}$ ) and for pure lipid bilayers ( $X \rightarrow 0$ ).

The micelle formation (Figure 9, m/w) is driven by a large entropy gain of  $-T\Delta s \approx -45$  kJ/mol. With the value of  $-T\Delta s/n_H = 1.7$  kJ/mol reported by Gill and Wadsö<sup>21</sup> for the solution of hydrocarbons in water, we would suppose an entropy gain of about  $-T\Delta s \approx -35$  kJ/mol considering a reasonable value of  $n_H = 21$ . Obviously, the remaining about  $-10$  kJ/mol are caused by headgroup effects. Indeed, a release of sorbed water from the headgroup, which can be concluded from the endothermic transfer heats of about  $+10$  kJ/mol, should be accompanied by an entropy gain. We note that the enthalpic and the entropic effects of the headgroup dehydration compensate each other to a large extent, so that the corresponding standard chemical potential change reflects mainly the contribution of the hydrophobic effect, which is merely entropic at 25 °C. The headgroup dehydration upon micelle formation is almost independent of the number of EO groups per detergent,  $n$ ,

because the varying molecular shape is matched by varying micellar shape and size to a large extent.

The standard chemical potential differences for the incorporation of detergent monomers into pure lipid membranes (Figure 9, b/w, ●) are very similar to the values for the micelle formation. This is compatible with the suggestion that its main source is the entropy gain due to the hydrophobic effect. In contrast to the micelle formation there is a considerable dependence of the transfer heats (▲) on  $n$ . As outlined in sections 4.1 and 4.2, this is caused by the curvature strain induced by the more or less cone-shaped detergents ( $n > 4$ ) leading to a gradual dehydration of all EO groups which are exposed to the lateral packing pressure in the membrane. Thus, one can conclude from the linearity of the thermodynamic transfer potentials with  $n$  that all the fourth until the eighth EO group per detergent are exposed to the same lateral packing pressure.

The data describing the detergent transfer from micelles to bilayers (Figure 9, b/m) represent just the differences of the respective b/w minus m/w data. Both the aggregates differ in their thermodynamic potential much less than aggregates from monomers, please note the change in ordinate scaling.

The transfer enthalpies (▲, △) reflect directly the curvature strain in the membrane, which is proportional to  $n$  for the truncated cone-shaped detergents ( $n \geq 5$ ) and close to zero for the cylindrical detergents ( $n = 3, 4$ ). For each detergent  $n \geq 5$ , the curvature strain is relieved with increasing detergent content (cf. ▲ and △) due to the well-known membrane fluidizing effect of the detergent.<sup>5-7,24</sup>

The standard chemical potential differences ( $\Delta\mu^\circ_{\text{D}^{\text{b/m}}}$ , cf. Figure 9, b/m, ●, ○) could be explained qualitatively in terms of the hydrophobic effect. The hydrocarbon chains of the detergents with low  $n$ , which do not strongly disturb the relatively tight packing in the lipid membrane, should be less exposed to water compared to the micellar state, yielding a negative  $\Delta\mu^\circ$ . For higher  $n$  and higher detergent contents  $X_e$  (cf. ○) the water exposure of the hydrocarbon chains in the membrane becomes larger ( $\Delta\mu^\circ$  increases) because of the detergent-induced membrane fluidization. However, we cannot exclude also headgroup effects to contribute to the  $\Delta\mu^\circ$  values observed.

**4.4. Intermediate Structures Close to the Membrane Saturation?** The heat  $q_{\text{D}^{\text{b/m}}}(X_e)$  for the transfer of  $\text{C}_{12}\text{EO}_8$  from micelles to bilayers was found to obey eq 1 very well within the complete lamellar range, i.e., from pure lipid membranes ( $X_e \rightarrow 0$ ) up very close to  $X_{\text{sat}}$  (at 25 °C).<sup>2</sup>

For higher temperature ( $T \geq 50$  °C) and other detergents ( $n \leq 6$ ) it has been found that close to the saturation composition  $X_{\text{sat}}$  the transfer heat  $q_{\text{D}^{\text{b/m}}}$  deviates from the model behavior according to eq 1. The three-stage model (bilayers, coexistence, micelles)<sup>3,4</sup> considering nonideal properties of detergent/detergent contacts<sup>2,8</sup> implies a vertical drop of the titration heat at  $X_{\text{sat}}$ , as has been found, e.g., for  $\text{C}_{12}\text{EO}_8$  and  $\text{C}_{12}\text{EO}_7$  at 25 °C in very good approximation and not a continuous decrease of the observed reaction heat over a wider concentration range. Various effects like, e.g., membrane rupture or vesicle destruction to large lamellar sheets have been reported to occur approaching the saturation composition of lipid/detergent-mixed membranes.<sup>24,28,29</sup> Such processes could be responsible for this effect observed.

**4.5. Lipid/Detergent Complex at Low Detergent Contents?** For  $T > 50$  °C or  $n \leq 6$ , an exothermic deviation of  $q_{\text{D}^{\text{b/m}}}(X_e)$  from the model of eq 1 (cf. points and lines in Figures 2, 4, and 5) is observed at low detergent contents  $X_e$ , which amounts up to about -2.5 kJ/mol for  $X_e \rightarrow 0$ . The local

maximum and change in sign of the observed heat of transfer are not comprehensible in terms of pair interactions, even if one would additionally consider<sup>27</sup> the tendency of the molecules in the mixture to form lipid-detergent contacts<sup>8</sup> instead of mixing randomly. Instead, the occurrence of the exothermic contribution must require cooperative interactions of more than two molecules or depend on general bilayer properties as fluidity, elasticity, etc.

Epand and Epand<sup>10</sup> reported very similar effects for membranes of inversely cone-shaped lipids upon incorporation of low amounts of the cone-shaped surfactant lyso-PC. Accordingly, the first injection of lyso-PC to DOPC and MeDOPE at 35 °C yielded heats of about +1 and -1.7 kJ/mol, respectively, whereas at significant surfactant content  $X_e \approx 0.07$  the injections heats for both samples approach +1 kJ/mol.

In terms of Figure 6 one can qualitatively illustrate this effect as follows. If the molecular shapes of a detergent molecule and surrounding lipid molecules within a lamella fit together compensating the opposing curvature strains, an enthalpically favorable state is reached. Strongly asymmetric surfactant (lyso-PC) fits together with strongly asymmetric lipids (e.g., MeDOPE), and weakly asymmetric detergents (e.g.  $\text{C}_{12}\text{EO}_5$ ) fit to weakly asymmetric lipids (POPC).

In fact, this molecular arrangement of one  $\text{C}_{12}\text{EO}_n$  detergent molecule surrounded by lipid molecules leads to a tight packing, replacing water of the headgroup region by a direct lipid-detergent headgroup interaction. Thus, X-ray diffraction measurements of samples hydrated at 97% relative humidity<sup>28</sup> indicated a significant rigidization of a POPC membrane upon incorporation of small amounts of  $\text{C}_{12}\text{EO}_n$  ( $\text{C}_{12}\text{EO}_8$  at  $X = 0.09$ , for  $\text{C}_{12}\text{EO}_3$  even up to  $X = 0.17$ ). Volke et al.<sup>29</sup> stated direct POPC- $\text{C}_{12}\text{EO}_4$  headgroup interactions replacing water on the basis of NOESY measurements.

However, in contrast to molecular complexes in gel state membranes,<sup>30</sup> this enthalpically preferred arrangement does not lead to a significant deviation from random mixing in the liquid crystalline state. Instead, the effect vanishes very soon with increasing detergent content, when detergent-detergent interactions become statistically relevant.

## 5. Conclusions

1. The variations of the lamellar/micellar phase transition boundaries and the nonideal behavior in lipid/detergent mixed bilayers as a function of the temperature and of the detergent headgroup size can at least qualitatively be explained in terms of a rather simple geometric packing model.

2. At 25 °C, the heats of transfer of the detergents  $\text{C}_{12}\text{EO}_n$  between water, micelles, and bilayers are caused almost merely by changes in headgroup hydration, which reflect variations of the packing pressure.

3. For  $n = 3-6$  (at 25 °C) and for temperatures above 50 °C (for  $\text{C}_{12}\text{EO}_8$ ) systematic deviations from the three-stage model (bilayers, coexistence, micelles) considering nonideal lipid/detergent pair interactions have been observed. An exothermic deviation from this model of up to -2.5 kJ/mol at low detergent contents could be related to a specific, water replacing attraction between lipid and detergent headgroups.<sup>28,29</sup> Effects observed approaching the membrane saturation with detergent could reflect a number of processes (like, e.g., membrane ruptures) reported in the literature.<sup>24-26</sup>

**Acknowledgment.** This work was supported by the Deutsche Forschungsgemeinschaft (Vo 526/1-1, SFB 294, and INK 23/A1-1). A.B. acknowledges the support by the Fonds der Chemischen Industrie and the Biotechnology Research Program

of the State of Rhineland-Palatinate. We thank Mrs. Westphal for excellent technical assistance. Many thanks also to Matthias Keller for experimental cooperation. Furthermore, we are grateful to Prof. Klaus Beyer and to Prof. M. Kozlov for helpful discussions.

### Glossary

|                                 |  |
|---------------------------------|--|
| C <sub>12</sub> EO <sub>n</sub> | oligo(ethylene oxide) dodecyl ether                            |
| cmc                             | critical micelle concentration                                 |
| DOPC                            | dioleoylphosphatidylcholine                                    |
| EO                              | ethylene oxide   |
| EYPC                            | egg yolk phosphatidylcholine                                   |
| ITC                             | isothermal titration calorimetry                               |
| L <sub>1</sub>                  | isotropic phase (micelles, oil in water microemulsion)         |
| L <sub>2</sub>                  | isotropic phase (inverse micelles, water in oil microemulsion) |
| L <sub>α</sub>                  | liquid crystalline lamellar phase                              |
| LUV                             | large unilamellar vesicles                                     |
| lyso-PC                         | lysophosphatidylcholine  |
| MeDOPE                          | methyldioleoylphosphatidylethanolamine                         |
| OG                              | octyl glucoside  |
| POPC                            | palmitoyl oleoyl phosphatidylcholine                           |

### References and Notes

- (1) Heerklotz, H.; Lantzsch, G.; Binder, H.; Klose, G.; Blume, A. *Chem. Phys. Lett.* **1995**, 235, 517.
- (2) Heerklotz, H.; Lantzsch, G.; Binder, H.; Klose, G.; Blume, A. *J. Phys. Chem.* **1996**, 100, 6764.
- (3) Lichtenberg, D.; Robson, R. J.; Dennis, E. A. *Biochim. Biophys. Acta* **1983**, 737, 285.
- (4) Lichtenberg, D. *Biomembranes-Physical Aspects*; Shinitzky, M., Ed.; VCH: Weinheim, 1993; Vol. 1, pp 63–96.

- (5) Lantzsch, G.; Binder, H.; Heerklotz, H.; Wendling, M.; Klose, G. *Biophys. Chem.* **1996**, 58, 289.
- (6) Thurmond, R. L.; Otten, D.; Brown, M. F.; Beyer, K. *J. Phys. Chem.* **1994**, 98, 972.
- (7) Otten, D.; Löbbecke, L.; Beyer, K. *Biophys. J.* **1995**, 68, 584.
- (8) Heerklotz, H.; Binder, H.; Lantzsch, G.; Klose, G. *Biochim. Biophys. Acta* **1994**, 1196, 114.
- (9) Israelachvili, J. N. *Intermolecular and surface forces*; Academic Press: London; 1991; Vol. 2.
- (10) Epand, R. M.; Epand, R. F. *Biophys. J.* **1994**, 66, 1450.
- (11) Wiseman, T.; Williston, S.; Brandts, J. F.; Lin, L. N. *Anal. Biochem.* **1989**, 179, 131.
- (12) Le Maire, M.; Møller, J. V.; Champeil, P. *Biochem.* **1987**, 26, 4803.
- (13) Edwards, K.; Almgren, M. *J. Colloid Interface Sci.* **1991**, 147/1, 1.
- (14) Mitchell, D. J.; Tiddy, G. J. T.; Waring, L.; Bostock, T.; McDonald, M. P. *J. Chem. Soc., Faraday Trans. I* **1983**, 79, 975.
- (15) Nilsson, P.-G.; Wennerström, H.; Lindman, B. *J. Phys. Chem.* **1983**, 87, 1377.
- (16) Andelman, D.; Kozlov, M. M.; Helfrich, W. *Europhys. Lett.* **1994**, 25/3, 231.
- (17) Paternostre, M.; Meyer, O.; Grabielle-Madelmont, C.; Lesieur, S.; Ghanam, M.; Ollivon, M. *Biophys. J.* **1995**, 69, 2476.
- (18) Vinron, P. K.; Talmon, Y.; Walter, A. *Biophys. J.* **1989**, 56, 669.
- (19) Partearroyo, M. A.; Alonso, A.; Goni, F. M.; Tribout, M.; Paredes, S. *J. Coll. Interf. Sci.* **1996**, 178, 156.
- (20) Vollmer, D.; Strey, R. *Europhys. Lett.* **1995**, 32/8, 693.
- (21) Gill, S. J.; Wadsö, I. *Proc. Natl. Acad. Sci. U.S.A.* **1976**, 73, 2955.
- (22) Paula, S.; Süss, W.; Tuchtenhagen, J.; Blume, A. *J. Phys. Chem.* **1995**, 99, 11742.
- (23) Olofsson, G. *J. Phys. Chem.* **1985**, 89, 1473.
- (24) Lasch, J. *Biochim. Biophys. Acta* **1995**, 1241, 269.
- (25) Ollivon, M.; Eidelman, O.; Blumenthal, R.; Walter, A. *Biochemistry* **1988**, 27, 1695.
- (26) Inoue, T.; Kawamura, H.; Okukado, S.; Shimozawa, R. *J. Colloid Interface Sci.* **1994**, 168, 94.
- (27) Cevc, G.; Marsh, D. *Phospholipid Bilayers*; Wiley: New York, 1985.
- (28) König, B.; Dietrich, U.; Klose, G. *Langmuir*, in press.
- (29) Volke, F.; Pampel, A. *Biophys. J.* **1995**, 68, 1960.
- (30) Mädler, B.; Klose, G.; Möps, A.; Richter, W.; Tschierske, C. *Chem. Phys. Lipids* **1994**, 71, 1.